Theta-phase dependent neuronal coding during sequence learning in human single neurons.

Leila Reddy[1,2 *+$], Matthew W. Self[3*] , Benedikt Zoefel[1,2], Marlène Poncet[1,2], Jessy K. Possel[3], Judith C. Peters[3,4], Johannes C. Baayen[5], Sander Idema[5], Rufin VanRullen[1,2], Pieter R. Roelfsema[3,6,7].

[*] Equally contributing authors
[+] Corresponding author
[$] Lead Contact

[1]Université de Toulouse, Centre de Recherche Cerveau et Cognition, Université Paul Sabatier, 31052, Toulouse, France.
[2]CNRS, UMR 5549, Faculté de Médecine de Purpan, 31052 Toulouse, France.
[3]Department of Vision and Cognition, Netherlands Institute for Neuroscience (KNAW), 1105 BA, Amsterdam, The Netherlands.
[4]Department of Cognitive Neuroscience, Faculty of Psychology and Neuroscience, Maastricht University, 6200 MD Maastricht, The Netherlands.
[5]Amsterdam University Medical Centers, location VUmc, Departments of Neurophysiology and Neurosurgery, Amsterdam, The Netherlands
[6]Department of Integrative Neurophysiology, Centre for Neurogenomics and Cognitive Research, Vrije Universiteit, 1081HV, Amsterdam, The Netherlands.
[7]Psychiatry Department, Academic Medical Center, 1105 AZ Amsterdam, The Netherlands

Abstract:

The ability to maintain a sequence of items in short-term memory (STM) is a fundamental cognitive function. Sequential item encoding in STM has been linked to a spike-theta-phase code for sequentially organized spatial locations observed in the rodent hippocampus (phase precession). The timing of neuronal activity relative to different brain oscillations is postulated to play a key role in maintaining the sequence order. We recorded single neuron and local field potential activity in the human brain during a sequence-learning task. Spikes for two consecutive items in the sequence were phase-locked at distinct phases of the theta oscillation. Surprisingly, the order of phases in the sequence-learning task was the opposite of that observed in phase precession during navigation. These results suggest that a spike-phase code is employed in the human brain during sequence learning, but with important differences compared to the rodent spike-theta-phase-dependent coding scheme.

Introduction:

Learning to memorize and maintain a sequence of items in short-term memory (STM) is fundamental for successful behavior. At the cellular level, this process is linked to sustained firing activity of individual neurons during the delay period between two stimuli (Fuster and Alexander, 1971; Konecky et al., 2017; Kornblith et al., 2017), as well as by anticipatory activity before the onset of an expected stimulus (Reddy et al., 2015). Short-term memory processes are also linked to various brain rhythms (Fuentemilla et al., 2010; Raghavachari et al., 2001), and there is converging evidence that neuronal firing activity during short-term memory can be timed (or phase-locked) to underlying theta oscillations. In humans, the strength of theta phase locking is predictive of human memory strength (Rutishauser et al., 2010) and navigational goals (Watrous et al., 2018). In rodents, spiking activity of place cells (O'Keefe and Dostrovsky, 1971) is locked to specific phases of the theta rhythm during spatial navigation. As a rat navigates through a sequence of spatial positions, place cells that represent each of these locations fire at distinct phases of the underlying theta rhythm, where spikes of a neuron occur at increasingly early phases as the rat approaches its place field. This process has been called phase-precession and has been proposed to play an important role in the learning of a sequence of spatial positions in the rodent brain (Buzsaki and Tingley, 2018), and by extension, in the encoding and maintenance of any ordered list in STM (Lisman and Jensen, 2013).

Here we asked whether a phase-dependent coding scheme is also observed in the human brain during sequence learning. Because humans are more visual creatures than rodents, we assumed that learning a sequence of visual objects could be analogous to learning a sequence of spatial positions in rodents. We hypothesized that theta phase could play an important role in stimulus encoding, and that the phase at which a given cell fires would vary with stimulus identity and order. In other words, while subjects are involved in learning a stimulus sequence, each item in the sequence might be represented by neuronal activity that is locked to a different theta phase. Will medial temporal lobe (MTL) neurons in human subjects that navigate a conceptual space defined by a sequence learning task, exhibit the same form of phase precession that has been observed in rodents during navigation?

Do MTL neurons also fire at increasingly early phases when the subject approaches the concept that activates the cells?

Results

To create an analogy with the navigation of spatial positions in rodents, we designed a conceptual space that consisted of a sequence of images. The viewers' subjective impression in this conceptual space was that the images were displayed on the rim of a rotating "wheel" that moved in the clockwise direction. The wheel moved forward smoothly during the inter-stimulus interval (ISI; 0.5 seconds), during which period, a gray placeholder covered all the images. At the end of the ISI period, the wheel stopped for 1.5 seconds, and the placeholder at the topmost position of the wheel was replaced by the next image in the sequence (Figure 1). On 20% of trials, instead of presenting the next stimulus, observers were presented with two choice stimuli and had to indicate which stimulus was the next in the sequence. In our previous work with the same paradigm (Reddy et al., 2015), we showed that, as a result of sequence learning, human MTL neurons that initially responded to a particular ("preferred") image on the wheel, started firing in anticipation of their preferred image, during the immediately preceding stimulus and the intervening ISI. This finding is reminiscent of rodent place cells that show anticipatory activity in sequentially ordered spatial environments (Mehta et al., 1997). In the current study, we ask whether theta-phase coding mechanisms observed in rodent place cells, are also observed while humans navigate this conceptual space. In other words, are different stimuli on the wheel assigned a particular theta phase for firing, and is the order of theta phases similar to that observed in rodents?

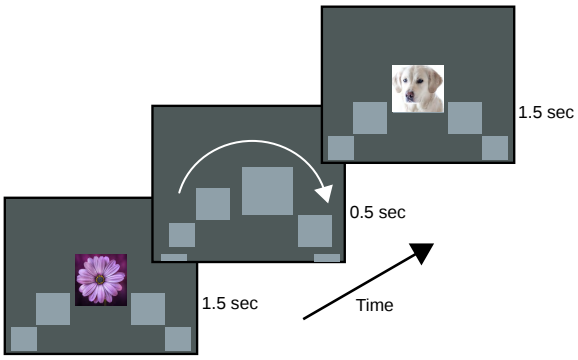

Figure 1: Experimental Design. In the sequence learning experiment, a sequence of 5-7 images was presented to the subjects in a fixed order. The sequence contained one preferred image for a selective neuron; the other images in the sequence were non-preferred images for this neuron. Each image was presented for 1.5s followed by an ISI of 0.5s. During the image presentation period (1.5s), an image was presented at the center of the screen, flanked by gray placeholders. During the ISI period, a placeholder replaced the central image, and all the placeholders moved in the clockwise direction. At the end of the ISI period, the central placeholder was replaced by the next image in the sequence. The sequence was repeated in this manner 60 times in each experimental session.

Nine human subjects learned the order of a number of stimuli presented in a pre-defined sequence, while we recorded spiking and LFP activity from the hippocampus, parahippocampal gyrus, and temporal cortex. Subjects rapidly learned the sequence order (>90% performance on test trials within 6 sequence presentations (Reddy et al., 2015)), and consequently all trials were included in the analyses described below. In prior screening sessions we identified neurons that had a strong preference for a particular stimulus (i.e., the neuron's preferred stimulus). The subsequent sequence-learning paradigm was designed to include this preferred stimulus, together with 4-6 non-preferred stimuli. In particular, we ensured that the stimulus prior to the preferred stimulus in the sequence (hereafter referred to as the preceding stimulus) was a non-preferred stimulus of the cell, although sequence learning caused a moderate increase in the spiking responses to the preceding stimulus, as mentioned above (Reddy et al., 2015). Here, we compare the theta-phase of firing for the preceding and preferred stimuli and determine whether the newly learned neuronal responses elicited by the preceding stimulus are encoded at a distinct theta phase relative to the responses elicited by the preferred stimulus.

In accordance with previous studies (Bohbot et al., 2017; Kraskov et al., 2007; Rutishauser et al., 2010; Watrous et al., 2018), we observed prominent theta activity in the 6-10Hz range in the local field potential (LFP) (Figure 2A, Figure S1A). To determine whether spiking activity of the neurons was phase-locked to these theta oscillations during the sequence-learning task, we computed the pairwise phase consistency (PPC) (Vinck et al., 2010). To improve the reliability of the PPC measure, we included all neurons from both the screening and sequence-learning sessions with firing rates >=~0.5Hz and that showed a selectivity to at least one stimulus (Figure 2B, *N*=93; see methods for PPC estimation). To estimate the significance of the PPC, we simulated a baseline null (no phase-locking) condition by time-reversing the entire LFP (but not the spike times), and re-computing the

PPC between spikes and the time-reversed LFP. This manipulation destroyed any spike-phase locking with the LFP but maintained the correlations inherent within the spike trains and LFP signals. The true PPC was significantly greater than the null condition at all frequencies below 25Hz (Rank-Wilcoxon test, $p < 0.0018$, Bonferonni corrected for the number of frequencies tested). In addition to the common (and expected) 1/f decrease in PPC across frequencies, a distinct peak of phase locking was observed in the 6-10 Hz theta range.

In the main experimental sequence-learning (SL) sessions, we recorded from 249 neurons, of which 63 showed a selective response to a preferred stimulus. The distribution of phase preferences in the theta range of these neurons that showed a selective response to a preferred stimulus (*N*=63) during the SL sessions is shown in Figure 2C (see Figure S1 B, C for phase preferences in the screening sessions). On average the ratio of spikes fired at the preferred versus the least preferred phase of the theta oscillation was 1.5 in the sequence-learning sessions (Figure 2D), which is indicative of a pronounced influence of theta phase on the neuronal firing rate.

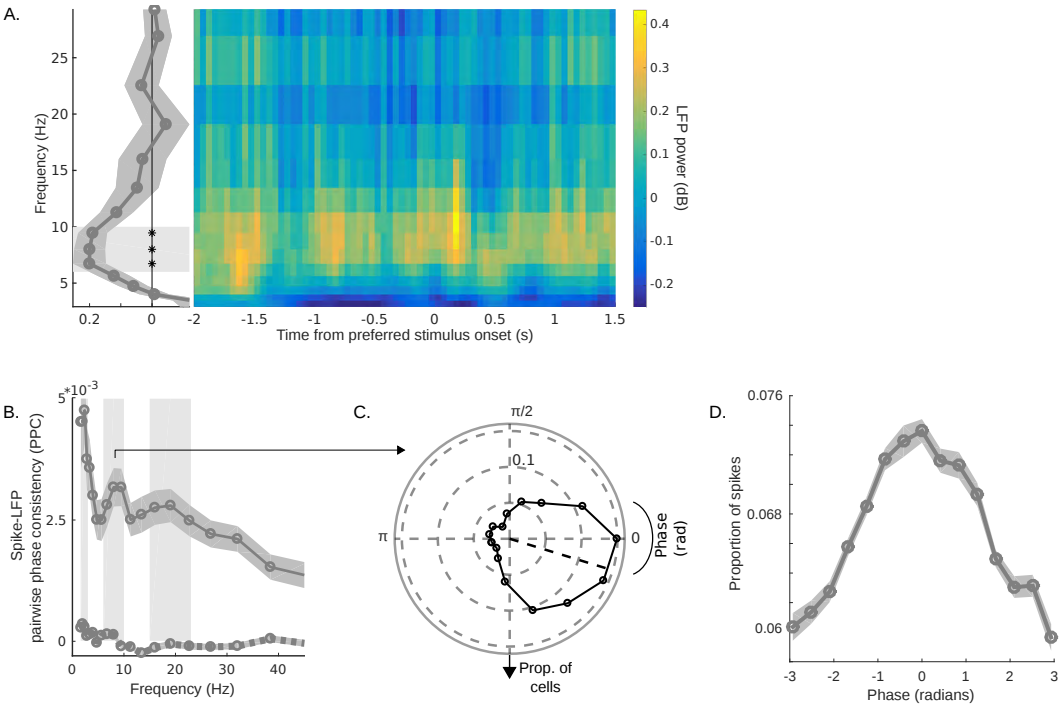

Figure 2: Theta phase-locking of neurons. A) LFP-power (left) and time frequency map (right) of the local field potentials recorded during the sequence-learning task. The power of the local field potential (LFP) relative to a 1/f fit is shown here in decibel units (see methods). In the right panel, time 0 corresponds to the onset of the preferred stimulus. The stimulus durations were 1.5s, with an ISI of 0.5s between stimuli. The preceding stimulus onset was thus at -2s. The panel on the left is the average LFP power, collapsed over the time axis of the plot on the right. Shaded area is the *SEM* across neurons. The time frequency map shows a peak in the theta band (6-10Hz). Star symbols on the frequency axis indicate significance of a comparison against 0 (paired t-test, $p < 0.05$ Bonferroni-corrected for multiple comparisons). B) The spike-LFP pairwise phase consistency as a function of frequency, averaged over all cell-LFP pairs (*N*=93 during the screening and sequence-learning sessions; see methods). The PPC analysis revealed a peak of spike-LFP phase locking in the theta (6-10Hz) band. The dark shaded curves are the *SEM* over cells. The shaded gray vertical regions correspond to the three frequency bands investigated below: 1.6-3 Hz, 6-10 Hz and 15-23 Hz. The dotted gray line is the result of a control analysis in which the LFP was time-reversed. C) Distribution of preferred phases for all cells in the sequence learning sessions with respect to the 6-10Hz theta oscillation. D). Theta-band phase modulation of spikes for all stimuli in the sequence learning sessions. Each cell's phase distribution was centered by subtracting the (circular) mean phase from the phase of each spike. The resultant phase distribution was then binned for each cell, and averaged across cells. The ratio of spikes fired at the peak preferred phase versus the least preferred phase is 1.5. The shaded areas correspond to the standard error of the mean across cells. See also Figures S1 and S5.

The peak of phase locking in the theta range indicates that the neurons have a preferred phase of firing relative to the underlying theta oscillations. To determine whether the neurons encoded the preceding and preferred stimuli at different phases of the theta cycle during sequence learning, we next compared the phase of firing for these two stimulus types (Figure 3A) over all 63 neurons that were selective for one of the stimuli in the sequence-learning sessions. The neurons showed

significant phase locking for both these stimulus types (p<0.0005, Rayleigh test). Importantly, the neurons fired at distinct theta phases for the preferred and preceding stimuli (mean angle ± SEM = -3°± 6° for the preferred and -55°± 6° for the preceding stimulus), with spikes elicited by the preceding stimulus occurring at an earlier phase of the theta cycle than those elicited by the preferred stimulus (Figure S2). The cell-wise paired difference between the phase preferences for these two stimulus types was significant across cells (F(1,125) = 10.5; p<0.005, Watson-William test; mean ± SEM = 58°± 6°; see Figure 3B, middle panel), indicating that the spikes fired in response to successive stimuli occurred at distinct phases of the theta rhythm. The difference of ~58° between the preceding and preferred phases corresponds to a time difference of ~20ms with respect to an 8 Hz oscillation. The phase-dependent stimulus encoding did not depend on the difference in the number of spikes fired to each stimulus (Figure S3), i.e. it does not seem to be caused by differences in firing rates. It also seems unlikely that the phase difference was caused by a phase reset evoked by stimulus onset, because the phase locking was relatively constant for the full duration of the stimulus (1.5s). The absence of an influence of phase-reset was confirmed with a control analysis in which we removed precisely stimulus-locked spikes (see Figure S4 and Methods).

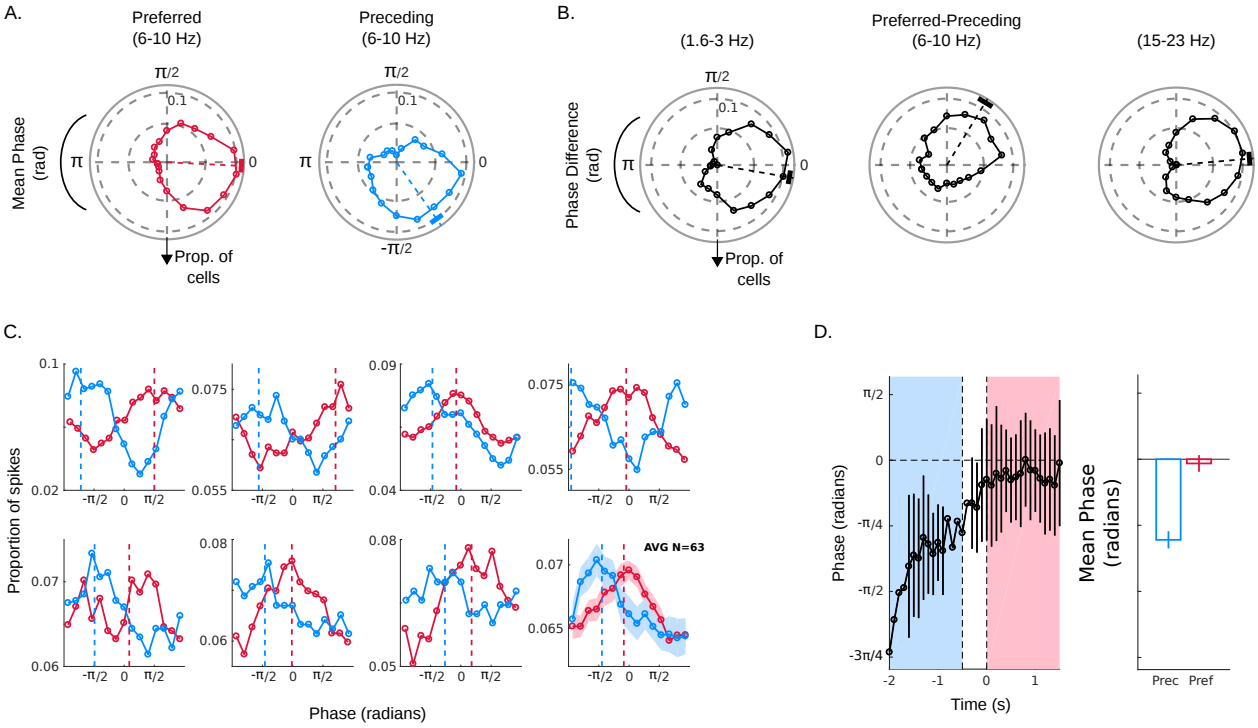

Figure 3: Phase encoding of successive stimuli in the MTL. A) Phase histogram of the phase of spiking relative to the theta band LFP for the preferred (red) and preceding (blue) stimuli across cells (N=63). The phase distributions were significantly different from the uniform distribution, indicating phase locking (p <0.0005 for both stimulus types, Rayleigh test). The dashed colored lines correspond to the mean phase, and the red and blue angular lines correspond to the *SEM* across cells. The phase distributions have been smoothed for display purposes (see Methods), but the mean phase (dashed lines) is calculated on unsmoothed data. B) Phase histogram of the cell-wise difference of phases at which the cells fired for the preferred and preceding stimuli in three frequency bands. The difference was significant (Watson-William test, p <0.005*)* only in the theta band. The dashed lines represent the mean phase, and the angular black lines correspond to the *SEM* across cells. C) Examples of histograms of phase of spiking relative to the theta band for individual cells and the average across cells (lower right). The blue curves are for the preceding stimuli and the red curves for the preferred stimuli. In the average plot, the shaded area is the *SEM* across cells. The dashed vertical lines indicate the mean phases. The difference between the distributions was significant at p < 0.005; Watson-William test for all panels. D) *left:* Change in mean phase across cells as a function of time. T=0 corresponds to the onset of the preferred stimulus. There was an ISI of 0.5s prior to the preferred stimulus (between the two dashed lines); the onset of the preceding stimulus occurred at -2s. Error bars represent the 95% confidence interval of the mean across cells, and are only plotted in time bins during which there was significant phase-locking (Rayleigh test, p<0.05). A linear fit through the phase values across time (-2s to 1.5s) revealed a strongly positive slope (slope = 21.8 deg/s, r^2 = 0.81, p <0.0005). *right:* Mean ± SEM of the phase during the preceding and preferred periods of the left panel. The data in the left panel has been smoothed for display purposes; the mean phases in the right panel are the true phases calculated within each time period, without smoothing. The phase difference in this figure is identical to that in panel C (average across cells). See also Figures S2, S3 and S4.

The PPC analysis indicated significant phase locking at a range of frequencies below 25Hz. In addition to a peak of PPC in the 6-10Hz range, we found two additional peaks of PPC in the delta (1.6-3Hz) and beta (15-23Hz) ranges (Figure 2B). To determine whether the phase-dependent stimulus coding observed in Figure 3A was specific to the theta band, or if it also occurred in other frequency bands, we repeated the analysis in the delta and beta bands. The difference in phase preference for the preferred vs. the preceding stimuli in all three frequency bands is shown in Figure 3B. The phase-dependent stimulus encoding was only significant in the theta band ($F(1,125) = 10.5$; $p<0.005$, Watson-William test; mean ± SEM = 58°± 6°; delta: $F(1,125) = 0.0002$; $p=0.98$, -10°± 5°; beta: $F(1,125) = 2.5$; $p=0.12$, 5°± 5°). In all subsequent analyses, we thus focus on the theta band. Figure 3C shows examples of phase-dependent stimulus encoding in seven representative individual neurons. Finally, to examine how the preferred phase evolved over a finer time scale as the sequence progressed from the preceding to the preferred stimuli, we plotted the mean phase across cells as a function of time (Figure 3D). This figure clearly shows the distinct phase-of-firing during the two time periods in which the stimuli were presented ($F(1,125) = 10.5$; $p<0.005$, Watson-William test), as well as the transition over time. A linear fit through the phase values across time (-2s to 1.5s) revealed a strongly positive slope (slope = 21.8 deg/s, $r^2 = 0.81$, $p < 0.0005$), again confirming the transition from one phase value to another across the two stimulus periods.

A.

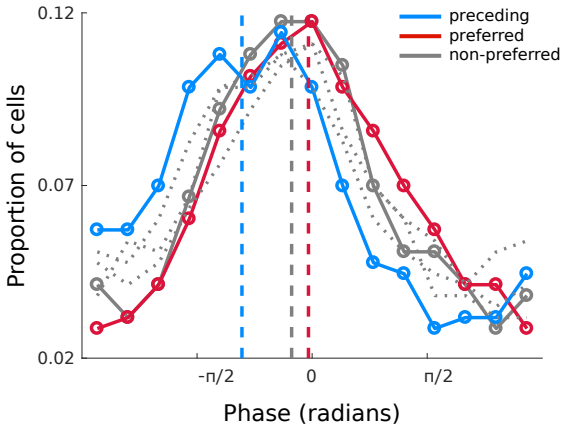

Figure 4: A) Phase distribution for the preferred (red), preceding (blue), and other non-preferred (gray) stimuli in the sequence. The vertical dashed lines correspond to the average phase of each distribution. The dotted gray lines correspond to the phase distributions for the three non-preferred stimuli shown individually. The cells showed significant phase locking for all three stimulus types ($p<0.005$, Rayleigh test).

Finally, we looked at the theta phase preference for the three other non-preferred stimuli in the sequence (i.e., if the preferred stimulus is stimulus N, we consider stimuli N-2, N+1 and N+2; Figure 4). The neurons showed significant phase locking with respect to the theta oscillation for the three non-preferred stimuli ($p < 0.0005$, Rayleigh test). The preferred phase for the non-preferred stimuli lay in between the preferred phases of the preferred and preceding stimuli (mean ± SEM = -16.02 °± 5.7°). A visual inspection of Figure 4 suggests that it is primarily the phase distribution of the preceding stimulus that is shifted compared to the largely overlapping distributions of the preferred and non-preferred stimuli. This observation was confirmed by a statistical analysis (Watson-William test, $p<0.05$ for preceding vs. non-preferred, $p = 0.4$ for preferred vs. non-preferred, and $p<0.005$ for preceding vs. preferred). We speculate that these observations suggest that the "default" phase preference of these neurons (i.e., the rhythmic influence of LFP oscillations that might be assigned to biophysical constraints, such as membrane potential fluctuations around the firing threshold) is reflected in the non-preferred stimuli. Indeed, the idea of a "default" phase is also suggested by the observation that the mean phase of the non-preferred stimuli was not significantly different from the mean phase computed over all the spikes fired in the screening sessions (screening mean ± SEM = -23.7 °± 6.7°; $F(1,111) = 0.2$; $p=0.66$; Figure S1B,C). The observed shift to ~-58° of the preceding stimuli phase distribution might then reflect a shift away from the "default" phase as a result of task-related learning of the preceding stimuli.

Discussion:

Our results provide evidence for phase-dependent neuronal coding during sequence learning in the human brain. Neuronal firing activity for the neurons' preferred and preceding stimuli in a sequence was phase-locked to the theta oscillation at distinct phases. Recent studies in human and non-human primates have investigated how a pair, or a series, of items during memory tasks is encoded in different brain regions. At the level of single neurons, it appears that the last presented item is the most reliably encoded in firing activity (Konecky et al., 2017; Kornblith et al., 2017), but these studies did not report phase locking to ongoing oscillations. Other studies have reported elevated theta-gamma phase-amplitude coupling (Bahramisharif et al., 2018; Heusser et al., 2016), or spike-phase coding with respect to higher frequency (32Hz) oscillations (Siegel et al., 2009). Influential models of phase-precession and STM however, posit a key role for a spike-based code phase-locked to theta rhythms, an assertion that we set out to test.

Although the exact role of oscillatory activity in sensory coding is still under debate (Histed and Maunsell, 2014), oscillatory activity in different frequency bands has been observed in relation with short-term memory (Lee et al., 2005; Lisman and Idiart, 1995; Pesaran et al., 2002; Siegel et al., 2009), attention (Buschman and Miller, 2007; Fries et al., 2001) and perception (Fiebelkorn et al., 2018; VanRullen, 2016). Spike-phase coding has also been observed in olfactory structures (Laurent, 2002), auditory cortex (Kayser et al., 2009), and during spatial navigation in humans (Watrous et al., 2018). Oscillations in the theta band in particular are thought to play an important role in the hippocampus. In rodents, phase precession is observed relative to a 7-9 Hz theta oscillation during spatial navigation (O'Keefe and Dostrovsky, 1971). Theta oscillations have also been observed in humans, in frequencies ranging from 3-9 Hz (Bohbot et al., 2017; Jacobs, 2014; Kraskov et al., 2007; Vass et al., 2016; Watrous et al., 2013; Watrous et al., 2018). Watrous et al., (2018) recently reported phase effects centered at lower theta frequencies (3Hz) for different navigational goals. However, unlike our study, that study did not report a consistent directionality of theta phase coding with respect to the navigational trajectory of the subject, a difference that might be due to the different theta frequency range, or the different task. To the best of our knowledge, a sequential spike-theta-phase code during sequence learning in humans has not been previously reported.

The encoding of sequential item information has been linked to the encoding of spatial locations in rodents during phase precession (Lisman and Jensen, 2013). Our results differ in important respects from findings regarding phase-precession in rodents during navigation. When a rodent approaches the place field of a neuron, the spikes are fired at successively earlier phases of the theta oscillation. One might therefore have predicted a gradual phase precession in the sequence-learning task, with spikes fired at successively earlier phases as the subjects approach the preferred stimulus of the cell. However, we found that the phases were generally similar across the stimuli in the sequence with one exception: spikes elicited by the stimulus that precedes the neurons' preferred stimulus fire at an earlier phase than the spikes elicited by the other stimuli in the sequence. In other words, we observed "phase succession" instead of phase precession during the transition from the preceding to the preferred stimulus (Figure 5A).

An important difference between our experimental setup and that used in rodents is the stimulus space that was explored. In rodents, the navigational space typically consists of running in repeated loops in a maze. Spatial navigation in virtual environments in humans has revealed that navigational goals are represented in the firing activity (Ekstrom et al., 2003), and phase-locking of MTL neurons (Watrous et al., 2018). However, these previous studies did not observe systematical differences in the phase of spikes elicited by a sequence of concepts. Here, we created a conceptual navigational space, which consisted of repetitive sequences of images. In this space, we find a distinct spike-phase code for the item that precedes the preferred item in the sequence. Can we reconcile our findings with theories of short-term memory that propose that different items are multiplexed at different phases of the theta rhythm (Lisman and Idiart, 1995)?

Standard theta-phase coding short-term memory (STM) models consider the encoding of a sequence of 5-7 stimuli (Jensen and Lisman, 1996; Lisman and Idiart, 1995), roughly equivalent to the capacity of 4-7 items in STM (Cowan, 2001; Luck and Vogel, 1997; Miller, 1956). Sequence encoding has been more broadly linked to the theta-phase coding of a sequence of 5-7 spatial locations in the rodent hippocampus (Buzsaki, 2010; Buzsaki and Moser, 2013; Eichenbaum et al., 1999; Lisman, 1999). Both coding schemes depend on the simultaneous responses of multiple neurons to different stimuli.

For example, in the rodent hippocampus, multiple place cells with overlapping receptive fields (place fields) fire at distinct phases within each theta cycle. Similarly, STM sequence coding models (Lisman, 2010) propose that multiple neurons with selectivity for different stimuli are simultaneously active during memory maintenance at distinct phases within a theta cycle. Our results differ from these models because we only observe significant neuronal responses for two stimuli at a time (the "preferred" stimulus of the neuron, and the stimulus "preceding" it in the sequence), despite having a larger number of items (5 to 7) in our sequences. One difference between rodent place fields and the conceptual representations in the human MTL is that the human MTL code may be sparser than the coding of spatial locations in rodents (Quiroga et al., 2005). Another difference may be related to our task, which did not require the subjects to hold all sequence items in memory. We only requested our subjects to make occasional judgments about the next item in the sequence, and these two special items (current and future) were associated with distinct phases in the theta cycle. We note, however, that a similar argument could be made about phase precession in place cells in the hippocampus, which also occurs without an explicit task to memorize the sequence of places visited by the animal.

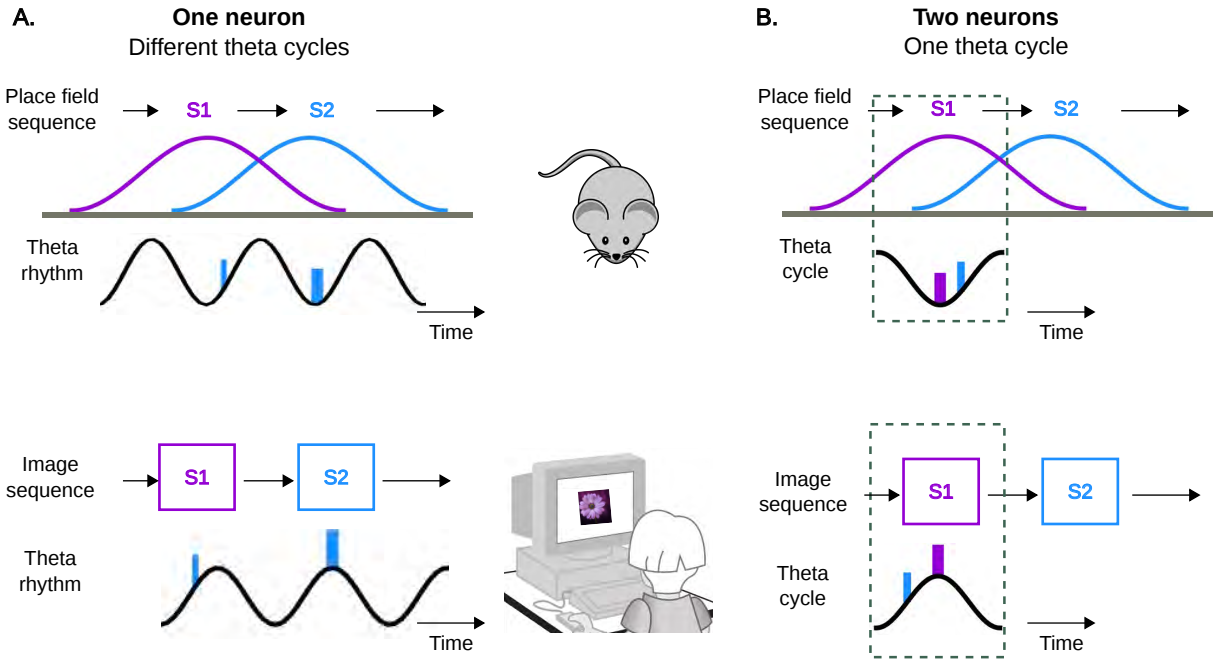

Figure 5: Comparison between spike-theta phase locking in rodents and humans. A). *(top)* In this example, a rodent navigates through a sequence of two spatial locations (S1 and S2). The theta-phase of firing of a single place cell, corresponding to S2 is shown here as a function of spatial position. The thickness of the bars corresponds to the strength of firing. Place cell S2 fires at a certain phase when the animal is at S1, and at an earlier phase (trough of the oscillation) when the rodent is in the center of place field S2. Modified from (Dragoi, 2013). *(bottom)* A human subject views a sequence of two images (S1 and S2). A neuron whose preferred stimulus is S2 fires at a late phase to S2 (peak of the oscillation, ~3°; see Figure 3 and Figure S2B), and at a relatively earlier phase to the preceding stimulus, S1. Thus, in the rodent, firing of S2 during the preceding stimulus S1 occurs at a later phase of the oscillation, whereas in our sequence-learning task, the spikes of S2 during the preceding stimulus S1 occur at an earlier phase (compared to spikes during the preferred stimuli).
B) Let us assume that while stimulus S1 is the preferred stimulus for one neuron, it is also the preceding stimulus for the neuron selective to S2. *(top)*.The firing activity of two place cells within one theta cycle, when the rodent is at S1: Place cell S1 fires at the earliest phase (trough) when the rodent is at the center of place field S1. At this moment, S2 fires at a relatively later phase. Thus, the order of spikes from S1 and S2 within one theta cycle reflects the temporal order in which the place fields will be traversed. *(bottom)* Firing activity of two neurons, selective to items S1 and S2 within one theta cycle, in our sequence-learning task. When S1 is presented on the screen, the neuron whose preferred stimulus is S1 fires at a late phase, near the peak of the oscillation. Stimulus S1 is also the preceding stimulus for the neuron whose preferred stimulus is S2. From Figure 3 we know that a cell's response to the preceding stimulus occurs at an earlier phase (~55°). Thus, in a given theta cycle, the two successive items are represented in the reverse order compared to the temporal order of the sequence.

Another important difference between our findings and place cells is in the order of spikes during the theta cycle. Theta-phase coding models (Jensen and Lisman, 1996) consider the response of multiple neurons (with distinct stimulus selectivity) within a single theta cycle (e.g., when the rat is at a particular spatial position). The behavior of multiple neurons coding for a given stimulus or place is typically inferred from single-unit recordings, by assuming that while one neuron codes a given stimulus as its preferred stimulus, another neuron codes the same stimulus as the one preceding its

own preferred stimulus (Figure 5). With this assumption in mind, we can ask about the order of all items within a single theta cycle, while the subject is at a particular location within a sequence of stimuli or places. In rodent navigation, the place cell with the earliest phase (trough of the oscillation) is the one with the place field at the animal's location, and the neurons with place fields that will be reached later fire at later phases. In our study however, the order is reversed, because the currently visible item has a later phase than the upcoming stimulus (Fig. 5B).

While this reversed representation within a theta cycle is intriguing, it is also worth noting that initial implementations of STM models (Lisman and Idiart, 1995) predicted precisely this reverse order for the spike-phase code. Furthermore, reverse temporal orders are also observed in the rodent hippocampus during awake or resting replay (Diba and Buzsaki, 2007; Foster and Wilson, 2006). Nevertheless, the importance of phase coding is still under dispute, given that some species, such as bats, have excellent navigational capabilities and similar neuronal place coding strategies, which do not depend on the theta rhythm (Buzsaki and Moser, 2013; Ulanovsky and Moss, 2007; Yartsev et al., 2011). The precise role of theta-phase coding therefore remains to be determined. Hence, it is encouraging that it is now possible to systematically study theta phase-coding in the human brain so that future studies can also use this approach to test the generality of theta-phase shifts during sequence coding, navigation in real and conceptual spaces, STM, and other cognitive functions.

Conclusion

In summary, learning and maintaining the order of a series of inputs (e.g., items, spatial locations, odors) or events is crucial to successfully negotiating an environment. An accurate encoding of a sequence of ordered stimuli enables an organism to predict the future based on regularities learned in the past. Some authors have argued that the role of the hippocampus is to encode events that occur in a temporally organized sequence (Eichenbaum et al., 1999; Wallenstein et al., 1998). More generally, the hippocampus may structure incoming information by generating sequentially organized cell assemblies, each for a different input or event; in this scheme, the theta rhythm is postulated to organize these assemblies into meaningful sequences (Buzsaki, 2010; Buzsaki and Tingley, 2018). Our results are broadly consistent with these hypotheses in that we observe distinct theta phase firing for two successive items in a sequence. However, we also report important differences between theta-phase encoding of sequential information in humans compared to place coding in rodents, raising interesting questions for future research.

Methods

Participants were nine patients (four female, age range 18-36 years) with pharmacologically intractable epilepsy undergoing epileptogical evaluation at the Amsterdam University Medical Centers, location VUmc, The Netherlands. Patients were implanted with chronic depth electrodes for 7-10 days in order to localize the seizure focus for possible surgical resection (Engel et al., 2005; Fried et al., 1997). All surgeries were performed by J.C.B and S.I. The Medical Ethics Committee at the VU Medical Center approved the studies. The electrode locations were based entirely on clinical criteria. Each electrode consisted of eight microwires from which we recorded single/multi-unit activity and local field potentials, and a ninth microwire that served as a local reference. The signal from the microwires was recorded using a 64-channel Neuralynx system, filtered between 1 and 9000 Hz, sampled at 32KHz. On average, each patient was implanted with 34 ± 11.8 microwires. Participants sat in their hospital room at the Epilepsy Monitoring Unit, and performed the experimental sessions on a laptop computer. All patients participated in the two types of experimental sessions described below.

Screening Sessions: Each day the patients first performed a screening session during which they were presented with a large variety of different images (famous people, relatives, animals, landmarks, objects etc.). Each image subtended 1.5 degrees of visual angle, and was presented at the center of the screen. Images were presented for 1000ms, followed by an inter-stimulus interval of 500ms. Each image was repeated 8 times in a randomized order. Between 7 and 51 images were used in the screening sessions depending on the availability of the patient. After the presentation of each image the patients performed a simple yes/no task, for example "Did the picture contain a human face"? The exact question depended on the picture set. This task ensured that patients attended to the stimuli. Data from the screening sessions were rapidly analyzed to determine which images were the "preferred" images of the neurons. "Preferred" images were defined as those that elicited a significant (paired t-test, $p<0.05$) response during the stimulus presentation period compared to the preceding ISI.

Sequence Learning (SL) Sessions: Following the screening sessions, the patients performed a total of 27 sequence learning (SL) sessions. The SL sessions were designed using information from the screening sessions. In each SL session, subjects were presented with a sequence of 5-7 images, always in a pre-determined order such that a given image, A, predicted the identity of the next image, B, and so on. Subjects were asked to remember the order of the stimuli in the sequence. Each stimulus was presented for 1.5s with an inter-stimulus interval (ISI) of 500ms, resulting in individual trials of 2000ms (Figure 1). The SL sessions were designed such that in each sequence of 5-7 images, at least one image was the preferred image of one of our neurons. In the rare cases where the sequence consisted of more than one preferred image, only one of the preferred images was used in the subsequent analyses (in other words, the same neuron was never counted twice in an SL session). Additionally, in order to be included in subsequent analyses, the stimulus immediately preceding the preferred stimulus in the sequence was required to be a non-preferred image (i.e., it did not elicit a significant response during the screening session) for this neuron. The sequence was repeated continuously 60 times resulting in experimental sessions of ~10-14 minutes, not including time spent by the subject on test trials. 20% of trials were "test" trials in which, instead of being presented with the next image of the sequence, subjects were shown two images side by side and asked to decide (by pressing one of two keys on the keyboard) which of the two would be the next image in the sequence.

To further the impression of a sequence of images we used the following display arrangement (Figure 1): Each image was presented at the center of the screen while placeholders (empty gray squares) were presented to the left and right of the central image. At the end of the 1500ms presentation period, the central image was replaced by a gray placeholder and all the grey squares moved one “step” forward in a clockwise direction for the duration of the ISI, such that each placeholder eventually occupied the next placeholder position. At the end of the ISI the placeholder that now occupied the central position was replaced by the next image in the sequence. The viewer’s subjective impression at the end of the ISI interval was that the central image had been hidden, and then moved clockwise, while the central position was replaced by the next image in the sequence.

Spike Detection and Sorting: Spike detection and sorting were performed with wave_clus (Quiroga et al., 2004). Briefly, the data were band pass filtered between 300-3000Hz and spikes were detected with an automatic amplitude threshold (Figure S5). Spike sorting was performed with a wavelet transform that extracted the relevant features of the spike waveform. Clustering was performed using a super-paramagnetic clustering algorithm. As in a previous study (Reddy et al., 2015), the clusters were classified as single- or multi-units. Multi-unit clusters reflect the activity of several neurons that cannot be further differentiated due to a low signal to noise ratio. As in (Reddy et al., 2015), the classification between single- and multi-unit was performed visually based on: 1) the spike shape and its variance; 2) the ratio between the spike peak value and the noise level; 3) the ISI distribution of each cluster; 4) the presence of a refractory period for the single-units; i.e. fewer than 1% of spikes in a 3ms or smaller inter- spike-interval.

Data Analysis: All analyses were performed with custom-made Matlab scripts and the FieldTrip toolbox (Oostenveld et al., 2011).

Number of neurons and their locations: Over the nine patients we recorded from 249 neurons (single and multi-unit) in the left and right hippocampi, temporal cortices, parahippocampal cortices, and the amygdala in the sequence learning sessions. To identify neurons that elicited a visual response to one of the stimuli in the sequence-learning sessions, we identified visually selective cells based on a one-way ANOVA across the stimuli ($p<0.05$) and visually responsive cells based on a paired t-test of the response to all stimuli vs. the baseline response ($p<0.01$). In addition, cells that were identified as selective during the screening sessions were also targeted if, during the sequence learning session, the response to the stimulus period was significantly higher than during the baseline period (paired t-test, $p<0.05$). For all these cells we ensured that the cell did not elicit a response to the preceding stimulus in the sequence (paired t-test, $p>0.05$). 63 neurons from the sequence learning sessions were thus identified as having preferred images. Of the 63 neurons from the sequence-learning sessions, 37 were located in the hippocampus, four in the parahippocampal cortex (PHC), 18 in the temporal lobe, and four in the amygdala. The results reported in this study did not vary by brain region.

Estimation of theta-band oscillatory activity

All LFP analyses were performed with the FieldTrip toolbox in Matlab (Oostenveld et al., 2011). The LFP was recorded from the same microwires as the spiking activity. It was downsampled to a 1,000-Hz sampling rate and notch filtered using a second order Butterworth filter. For each channel, we computed the time-frequency decomposition for 28 different frequencies: $f = 2^x$ with $x \in \{6/8, 8/8, 10/8, \ldots 60/8\}$ (Rutishauser et al., 2010). The time frequency decomposition was performed with the multitaper method over a 3 second epoch encompassing the preceding and preferred stimuli of the raw LFP trace, using two cycles per time-window at each frequency. We estimated whether significant theta activity was present in the LFP by fitting a 1/f function to the power spectrum and taking the ratio (in units of decibels) between the actual power spectrum and the 1/f fit (Figure 2A). Significance was estimated with a t-test, Bonferroni corrected for multiple comparisons (28 frequencies). In addition to estimating theta power with the raw traces, we also measured the power spectrum of the oscillations around the time of each spike (spike triggered power; Figure S1A). We extracted a 1s LFP segment centered on each spike and extracted the frequency spectrum of each segment. The average power spectrum of these LFP traces was estimated by taking the average of the absolute values (the power) of the spectra of all LFP segments (Fries et al., 2001). The resultant power spectrum was fitted to a 1/f function, and the ratio (in decibel units) computed. Significance was estimated with a t-test, Bonferroni corrected for multiple comparisons over 28 frequencies (Figure S1A). Both measures of quantifying oscillatory power revealed prominent theta activity in the 6-10Hz range.

Estimation of spike-LFP phase-locking

The instantaneous LFP phase was estimated using a Hanning taper over the entire duration of the session (i.e., without epoching), using five cycles per time-window at each frequency. A phase of zero corresponds to the peak of the LFP oscillation, and a phase of ± 180 corresponds to the spike being at the trough of the oscillation (Figure S2B). Phase-locking was evaluated 1) with the pairwise phase consistency (PPC) measure (Vinck et al., 2010) for all neurons that showed a visual response to at least one stimulus during either the screening or sequence learning experiments, and 2) with the Rayleigh test. The PPC at each frequency is calculated by considering the cosine of the angular distance (or the dot product) between all pairs of phase vectors. The PPC is equal to the average dot product across all pairs of phase vectors. Negative PPC values correspond to angular distances greater than 90°. For the PPC analysis we considered neurons from both the screening and sequence learning sessions that (i) showed a visual response to at least one stimulus, and (ii) that fired >500 spikes (>=~0.5Hz firing rates over a ~15 minute session), to reduce variability in the estimation of the PPC. With these criteria, a total of 93 neurons from both the sequence learning and screening sessions were included in the PPC estimation. To estimate the significance of the PPC, we simulated a baseline null (no phase-locking) condition by time-reversing the entire LFP (but not the spike times), and re-computing the PPC between spikes and the time-reversed LFP. This manipulation destroyed any phase locking with the LFP but maintained any correlations inherent within the spike trains and LFP signals. The PPC analysis indicated 3 peaks of phase locking in the 1.6-3 Hz (delta range), 6-10 Hz (theta range) and 15-23 Hz (beta range). For subsequent analyses, the LFPs were therefore band-pass filtered with a second order Butterworth filter in these three frequency ranges. A phase value for each spike in each frequency range was extracted using the Hilbert transform on the band-passed signal. Phase values were assigned to each stimulus in the sequence depending on the time at which the spikes were emitted. In addition to the PPC, for each neuron, phase locking was also estimated by comparing the distribution of phase angles against the uniform distribution using the Rayleigh test.

Stimulus specific spike-phase-locking

To determine whether the spikes fired at different phases in response to the different stimuli, we assigned phase values to each stimulus depending on the time at which the spikes were fired. Phase values were binned into 15 bins. For visualization purposes only a smoothing of two bins in either direction was applied. To compare the phase distributions for different stimuli the Williams-Watson test from the Circular Toolbox for Matlab (Berens, 2009) was applied to the unsmoothed data.

To control for the effect of spike number on phase between the preferred and preceding stimuli (Figure S3), we equalized the number of spikes for each neuron by rejecting the highest firing rate trials for the preferred stimulus and the lowest firing rate trials for the preceding stimuli. This procedure was

performed progressively until the difference in the mean number of spikes for the two stimuli was less than 0.005. Finally, we re-computed the preferred phases for the preceding and preferred stimuli, while only considering the reduced number of trials.

Phase-Reset and Inter-trial Coherence (ITC)

The inter-trial coherence was computed at each time and frequency point (Figure S4). On each trial of the preferred and preceding stimuli we extracted an LFP segment in the time window of [-0.5 1.5] sec, with time 0 corresponding to stimulus onset. The phase and power at each time and frequency point was extracted from a time frequency transform of the signal. The parameters for the time-frequency transform are the same as described above: namely, the multi-taper method with 2 cycles per frequency on the notch-filtered and down sampled signal, at 28 frequencies, and in a time interval of -0.5s to 1.5s in steps of 50ms. The inter-trial coherence is the absolute value of the average spectrum normalized by its amplitude (Delorme and Makeig, 2004), and varies between zero (no phase-locking) and one (perfect phase-locking). Equal numbers of trials were used for the preferred and preceding stimuli.

Author Contribution: L.R and P.R.R designed the study. J.C.B and S.I performed the surgeries. M.S, B.Z, M.P, J.K.P, J.C.P and L.R. collected data. L.R analyzed the data with input from R.V. L.R. wrote the first version of the manuscript. L.R and P.R.R finalized the manuscript. All authors commented on the finalized version of the manuscript.

Acknowledgments: We are grateful to to C.J. Stam, E. van Dellen, L. Douw, P. Ris, S. Claus, D. Velis, and R. Joosten for help with obtaining ethics approval and for technical help with the patients and recordings. This work was supported by grants from the Fyssen foundation and the Université Paul Sabatier, Toulouse, France (BQR, 2009 and Appel à Projets de Recherche Labellisés, 2013) to L.R., the European Research Council (ERC Consolidator Grant P-Cycles number 614244) to R.V., the Studienstiftung des Deutschen Volkes (German Academic Scholarship Foundation) to B.Z., the European Union (ERC Grant Agreement n. 339490 ‘‘Cortic_al_gorithms’’ and grant agreements 720270 and 785907 ‘‘Human Brain Project SGA1 and SGA2’) and the Friends Foundation of the Netherlands Institute for Neuroscience to P.R.R.

References

Bahramisharif, A., Jensen, O., Jacobs, J., and Lisman, J. (2018). Serial representation of items during working memory maintenance at letter-selective cortical sites. PLoS biology 16, e2003805.
Berens, P. (2009). CircStat: A Matlab Toolbox for Circular Statistics. Journal of Statistical Software 31, 1-21.
Bohbot, V.D., Copara, M.S., Gotman, J., and Ekstrom, A.D. (2017). Low-frequency theta oscillations in the human hippocampus during real-world and virtual navigation. Nature communications 8, 14415.
Buschman, T.J., and Miller, E.K. (2007). Top-down versus bottom-up control of attention in the prefrontal and posterior parietal cortices. Science 315, 1860-1862.
Buzsaki, G. (2010). Neural syntax: cell assemblies, synapsembles, and readers. Neuron 68, 362-385.
Buzsaki, G., and Moser, E.I. (2013). Memory, navigation and theta rhythm in the hippocampal-entorhinal system. Nature neuroscience 16, 130-138.
Buzsaki, G., and Tingley, D. (2018). Space and Time: The Hippocampus as a Sequence Generator. Trends in cognitive sciences 22, 853-869.
Cowan, N. (2001). The magical number 4 in short-term memory: a reconsideration of mental storage capacity. Behavioral and Brain Sciences 24.
Delorme, A., and Makeig, S. (2004). EEGLAB: an open source toolbox for analysis of single-trial EEG dynamics including independent component analysis. Journal of neuroscience methods 134, 9-21.
Diba, K., and Buzsaki, G. (2007). Forward and reverse hippocampal place-cell sequences during ripples. Nature neuroscience 10, 1241-1242.
Dragoi, G. (2013). Internal operations in the hippocampus: single cell and ensemble temporal coding. Frontiers in systems neuroscience 7, 46.
Eichenbaum, H., Dudchenko, P., Wood, E., Shapiro, M., and Tanila, H. (1999). The hippocampus, memory, and place cells: is it spatial memory or a memory space? Neuron 23, 209-226.

Ekstrom, A.D., Kahana, M.J., Caplan, J.B., Fields, T.A., Isham, E.A., Newman, E.L., and Fried, I. (2003). Cellular networks underlying human spatial navigation. Nature 425, 184-188.
Engel, A.K., Moll, C.K., Fried, I., and Ojemann, G.A. (2005). Invasive recordings from the human brain: clinical insights and beyond. Nature reviews Neuroscience 6, 35-47.
Fiebelkorn, I.C., Pinsk, M.A., and Kastner, S. (2018). A Dynamic Interplay within the Frontoparietal Network Underlies Rhythmic Spatial Attention. Neuron 99, 842-853 e848.
Foster, D.J., and Wilson, M.A. (2006). Reverse replay of behavioural sequences in hippocampal place cells during the awake state. Nature 440, 680-683.
Fried, I., MacDonald, K.A., and Wilson, C.L. (1997). Single neuron activity in human hippocampus and amygdala during recognition of faces and objects. Neuron 18, 753-765.
Fries, P., Reynolds, J.H., Rorie, A.E., and Desimone, R. (2001). Modulation of oscillatory neuronal synchronization by selective visual attention. Science 291, 1560-1563.
Fuentemilla, L., Penny, W.D., Cashdollar, N., Bunzeck, N., and Duzel, E. (2010). Theta-coupled periodic replay in working memory. Current biology : CB 20, 606-612.
Fuster, J.M., and Alexander, G.E. (1971). Neuron activity related to short-term memory. Science 173, 652-654.
Heusser, A.C., Poeppel, D., Ezzyat, Y., and Davachi, L. (2016). Episodic sequence memory is supported by a theta-gamma phase code. Nature neuroscience 19, 1374-1380.
Histed, M.H., and Maunsell, J.H. (2014). Cortical neural populations can guide behavior by integrating inputs linearly, independent of synchrony. Proceedings of the National Academy of Sciences of the United States of America 111, E178-187.
Jacobs, J. (2014). Hippocampal theta oscillations are slower in humans than in rodents: implications for models of spatial navigation and memory. Philosophical transactions of the Royal Society of London Series B, Biological sciences 369, 20130304.
Jensen, O., and Lisman, J.E. (1996). Novel lists of 7 +/- 2 known items can be reliably stored in an oscillatory short-term memory network: interaction with long-term memory. Learning & memory 3, 257-263.
Kayser, C., Montemurro, M.A., Logothetis, N.K., and Panzeri, S. (2009). Spike-phase coding boosts and stabilizes information carried by spatial and temporal spike patterns. Neuron 61, 597-608.
Konecky, R.O., Smith, M.A., and Olson, C.R. (2017). Monkey prefrontal neurons during Sternberg task performance: full contents of working memory or most recent item? Journal of neurophysiology 117, 2269-2281.
Kornblith, S., Quian Quiroga, R., Koch, C., Fried, I., and Mormann, F. (2017). Persistent Single-Neuron Activity during Working Memory in the Human Medial Temporal Lobe. Current biology : CB.
Kraskov, A., Quiroga, R.Q., Reddy, L., Fried, I., and Koch, C. (2007). Local field potentials and spikes in the human medial temporal lobe are selective to image category. Journal of cognitive neuroscience 19, 479-492.
Laurent, G. (2002). Olfactory network dynamics and the coding of multidimensional signals. Nature reviews Neuroscience 3, 884-895.
Lee, H., Simpson, G.V., Logothetis, N.K., and Rainer, G. (2005). Phase locking of single neuron activity to theta oscillations during working memory in monkey extrastriate visual cortex. Neuron 45, 147-156.
Lisman, J. (2010). Working memory: the importance of theta and gamma oscillations. Current biology : CB 20, R490-492.
Lisman, J.E. (1999). Relating hippocampal circuitry to function: recall of memory sequences by reciprocal dentate-CA3 interactions. Neuron 22, 233-242.
Lisman, J.E., and Idiart, M.A. (1995). Storage of 7 +/- 2 short-term memories in oscillatory subcycles. Science 267, 1512-1515.
Lisman, J.E., and Jensen, O. (2013). The theta-gamma neural code. Neuron 77, 1002-1016.
Luck, S.J., and Vogel, E.K. (1997). The capacity of visual working memory for features and conjunctions. Nature 390, 279-281.
Mehta, M.R., Barnes, C.A., and McNaughton, B.L. (1997). Experience-dependent, asymmetric expansion of hippocampal place fields. Proceedings of the National Academy of Sciences of the United States of America 94, 8918-8921.
Miller, G.A. (1956). The magical number seven, plus minus two: some limits on our capacity for processing information. Psychological review 63, 81-97.
O'Keefe, J., and Dostrovsky, J. (1971). The hippocampus as a spatial map. Preliminary evidence from unit activity in the freely-moving rat. Brain research 34, 171-175.

Oostenveld, R., Fries, P., Maris, E., and Schoffelen, J.M. (2011). FieldTrip: Open source software for advanced analysis of MEG, EEG, and invasive electrophysiological data. Computational intelligence and neuroscience 2011, 156869.
Pesaran, B., Pezaris, J.S., Sahani, M., Mitra, P.P., and Andersen, R.A. (2002). Temporal structure in neuronal activity during working memory in macaque parietal cortex. Nature neuroscience 5, 805-811.
Quiroga, R.Q., Nadasdy, Z., and Ben-Shaul, Y. (2004). Unsupervised spike detection and sorting with wavelets and superparamagnetic clustering. Neural computation 16, 1661-1687.
Quiroga, R.Q., Reddy, L., Kreiman, G., Koch, C., and Fried, I. (2005). Invariant visual representation by single neurons in the human brain. Nature 435, 1102-1107.
Raghavachari, S., Kahana, M.J., Rizzuto, D.S., Caplan, J.B., Kirschen, M.P., Bourgeois, B., Madsen, J.R., and Lisman, J.E. (2001). Gating of human theta oscillations by a working memory task. The Journal of neuroscience : the official journal of the Society for Neuroscience 21, 3175-3183.
Reddy, L., Poncet, M., Self, M.W., Peters, J.C., Douw, L., van Dellen, E., Claus, S., Reijneveld, J.C., Baayen, J.C., and Roelfsema, P.R. (2015). Learning of anticipatory responses in single neurons of the human medial temporal lobe. Nature communications 6, 8556.
Rutishauser, U., Ross, I.B., Mamelak, A.N., and Schuman, E.M. (2010). Human memory strength is predicted by theta-frequency phase-locking of single neurons. Nature 464, 903-907.
Siegel, M., Warden, M.R., and Miller, E.K. (2009). Phase-dependent neuronal coding of objects in short-term memory. Proceedings of the National Academy of Sciences of the United States of America 106, 21341-21346.
Ulanovsky, N., and Moss, C.F. (2007). Hippocampal cellular and network activity in freely moving echolocating bats. Nature neuroscience 10, 224-233.
VanRullen, R. (2016). Perceptual Cycles. Trends in cognitive sciences 20, 723-735.
Vass, L.K., Copara, M.S., Seyal, M., Shahlaie, K., Farias, S.T., Shen, P.Y., and Ekstrom, A.D. (2016). Oscillations Go the Distance: Low-Frequency Human Hippocampal Oscillations Code Spatial Distance in the Absence of Sensory Cues during Teleportation. Neuron 89, 1180-1186.
Vinck, M., van Wingerden, M., Womelsdorf, T., Fries, P., and Pennartz, C.M. (2010). The pairwise phase consistency: a bias-free measure of rhythmic neuronal synchronization. NeuroImage 51, 112-122.
Wallenstein, G.V., Eichenbaum, H., and Hasselmo, M.E. (1998). The hippocampus as an associator of discontiguous events. Trends in neurosciences 21, 317-323.
Watrous, A.J., Lee, D.J., Izadi, A., Gurkoff, G.G., Shahlaie, K., and Ekstrom, A.D. (2013). A comparative study of human and rat hippocampal low-frequency oscillations during spatial navigation. Hippocampus 23, 656-661.
Watrous, A.J., Miller, J., Qasim, S.E., Fried, I., and Jacobs, J. (2018). Phase-tuned neuronal firing encodes human contextual representations for navigational goals. eLife 7.
Yartsev, M.M., Witter, M.P., and Ulanovsky, N. (2011). Grid cells without theta oscillations in the entorhinal cortex of bats. Nature 479, 103-107.